Alexander Ross

PHYS221

Project I

Determination of the Gamma Cross-Section of Aluminium

Introduction

In this experiment, we conducted basic research into the subject of cross-sections, and specifically the cross-section of Aluminium. A cross-section can be thought of as a measure of probability that a given physical phenomenon will occur as a consequence of the collision of photons (γ-particles) with matter particles in the target, which is determines how large the transverse area to the incident particles must be in order for a certain proportion of the photons to scatter. We will discuss the results of the experiment with radioactive Ba-133 as the source of these photons.

When the incident photons interact with the aluminium target, some of the photons pass through unimpeded, but many are scattered as a result of three principal phenomena. The first of these is Compton scattering, which refers to the process whereby an incoming photon is scattered inelastically by a charged particle (usually an electron), which may result in a loss of energy to the electron, thus causing the wavelength of the emitted light to differ from that absorbed. The second phenomenon that may occur in the interaction of photons with the target is the photoelectric effect. This process describes how an atom in the target absorbs an incoming photon, and subsequently emits an electron from its shell. As the electron was initially in a bound state in the atom, some of the energy absorbed from the incident photon is required to overcome the binding energy of the atom. This determines the work function of the material. This loss of energy will result in the emission of an electron with lower energy than the initial photon. The final process which may occur in the interaction of photons with the matter target is pair-production. By this phenomenon, the incoming photon passes near a massive nucleus and is converted to mass in the form of an electron-positron pair. In order for this process to occur, the photon must have at least twice the rest-energy of the created electron. There is an individual cross-section associated with each of these phenomena but we will only be concerned about the total cross-section given by their sum.

Methods

In order to arrive at a final value for the cross-section of our aluminium target, it was first necessary to calculate some preliminary values needed for the cross-section's final determination. The equation underlying these calculations was the following:

$$\sigma_T = \frac{1}{x\rho_A} ln(\frac{I_0}{I}) ,$$

where σ_T is the total cross-section, *x* is the thickness of the aluminium absorber, ρ_A is the density of the material through which the light passes, and I and I_0 refer to the measured and incident intensities of light. This can be reduced to the equation:

$$I(x) = I_0 e^{-x\mu_l} \text{ , with } \mu_l = \rho_A \sigma_T \text{ .}$$

Since ρ_A is a determined constant, All that was necessary to discover was the value of μ, which is called the mass attenuation coefficient for the material. In order to investigate the linear attenuation coefficient, we needed to make plots of the measured intensity (also later referred to by the count rate) of the light after passing through the aluminium absorber against the thickness of the absorber. Therefore it was necessary to vary the value of the thickness *x* in order to observe a relationship between the thickness of the absorber and the measured intensity. We first plotted the intensities against channel (explained in next section) to observe the patterns and identify the peaks of intensity. We then fitted the resulting data of absorber thickness versus intensity to an exponential decay curve in order to obtain the value of the linear attenuation coefficient from the graphs, and to thence be able to calculate the total cross-section for aluminium σ_T .

Set-Up

Over the four-week course of the experiment, we investigated aluminium's cross-section remotely via use of the Red Pitaya programme, an open-source hardware project, which got rid of the necessity for in-person data collection. To collect the relevant data, we used the following set-up. The radioactive source (in this case Barium-133) was held in the vicinity of the aluminium absorber and by the nature of its radioactive instability, consistently emitted gamma particles towards the absorber. Behind the absorber and in line with the radioactive Barium source a sodium Iodide (NaI) crystal was set up, doped with Thallium, which upon absorption of the gamma particles emitted a flash of light (scintillation) able to be received by the photomultiplier tube (PMT). The PMT has an electronic photon sensor which detects the sodium iodide's emission, and as a result produces a current via the photoelectric effect. As the name suggests, the PMT then multiplies this current to produce an electric pulse. The light produced in the scintillator passes through a glass window into the PMT where it liberates an electron by the photoelectric effect. When these electrons strike a dynode in the tube, many more electrons are emitted and subsequently accelerated to the next dynode. This process is repeated multiple times culminating in the PMT's output pulses. The pulses indicate the amount of energy of the incident photons and the pattern that these pulses create over time can be analysed to suggest what processes led to the photons' emission.

Data Analysis

The data that will be analysed were all taken using the Red Pitaya programme, and displayed by the multichannel analyser (MCA) in the pulse height analyser mode which sorted the pulses from the PMT into channels according to their amplitude. The Barium source was used to take eight sets of data - one for each thickness of the aluminium absorber (0, 0.5, 1, 2, 4, 8, 16, and 32 mm). Of the four energy peaks observed from the data, I was tasked with analysing the first two, and lowest energy, peaks (35keV and 81keV). First I made plots using the data from the MCA for each peak and for each thickness, and attempted to fit these data with Gaussian functions. The plots for x=32mm and x=16mm are shown below.

x=32mm:

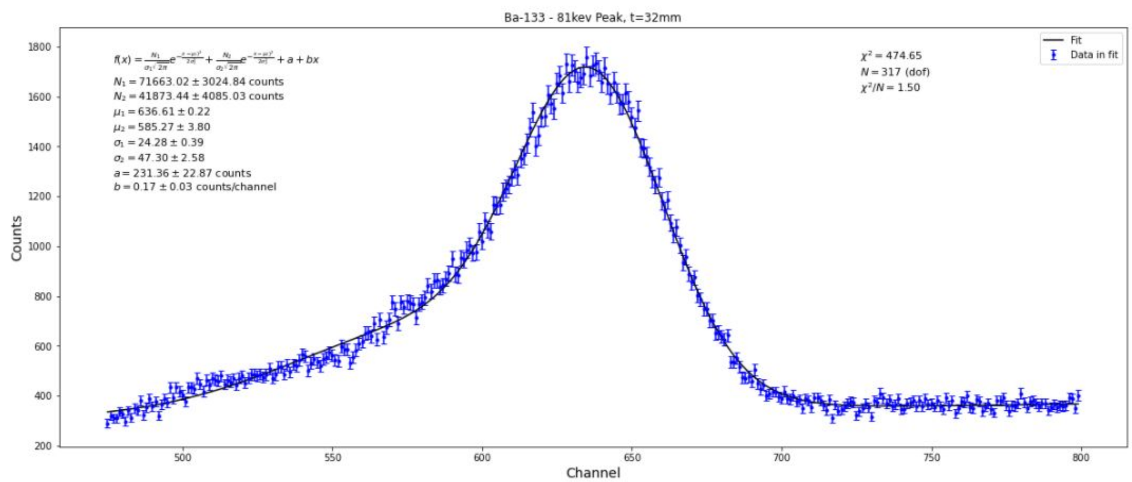

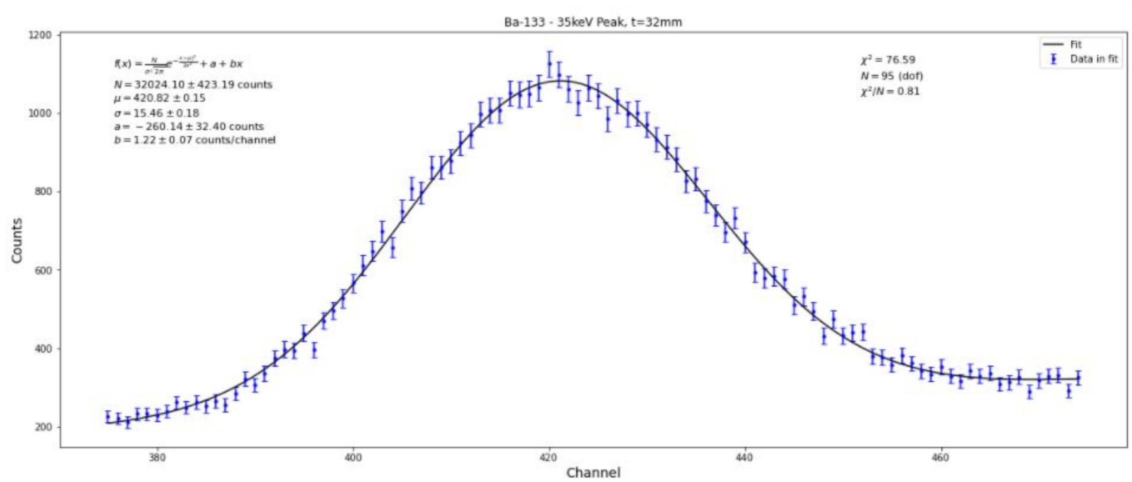

x=16mm:

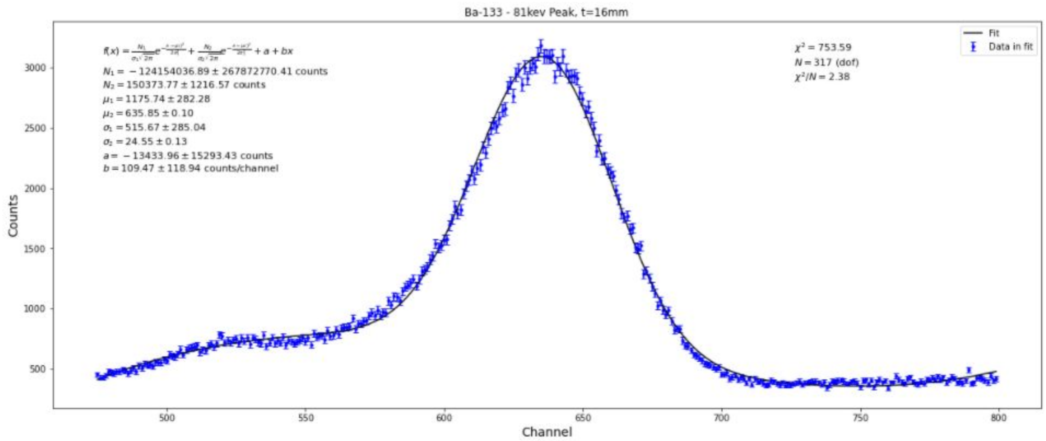

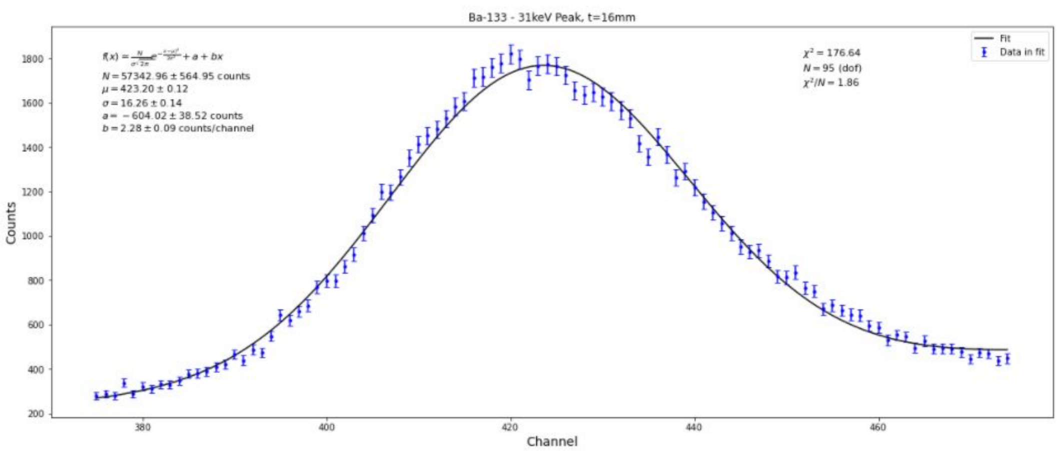

It can be seen from the graphs and from the chi squared/reduced chi squared values that the fitted Gaussian represents the data well for these thicknesses of the absorber. For the 35keV plot, $\frac{\chi^2}{N} = 0.81,\ 1.86$ and for the 81keV plots, $\frac{\chi^2}{N} = 1.50,\ 2.38$. It can also be seen that the count number increased for both peaks when the absorber's thickness was reduced, which was as expected. This was the case for every subsequent thickness. When fitting the data for very low thicknesses, however, the Gaussian distributions were not as accurate at representing the data as for the thicker absorbers:

x=0.5mm:

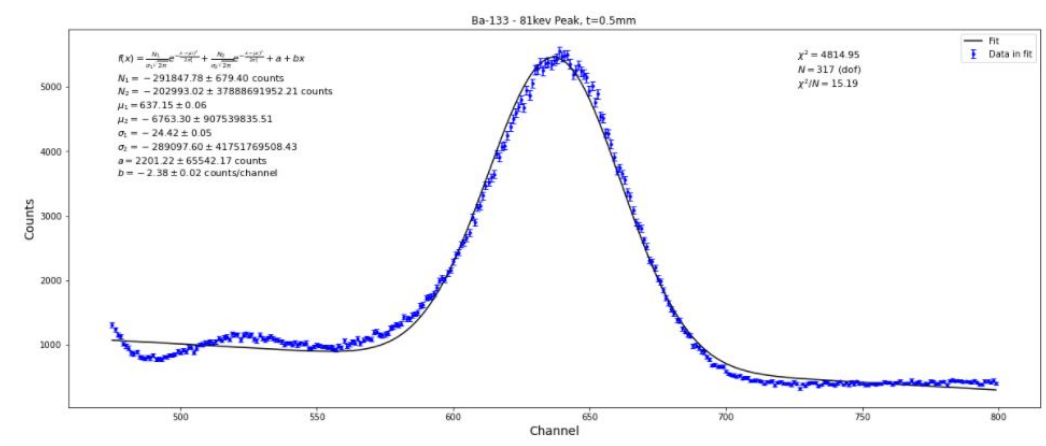
Ba-133 - 81kev Peak, t=0.5mm
$N_1 = -291847.78 \pm 679.40$ counts
$N_2 = -202993.02 \pm 37888691952.21$ counts
$\mu_1 = 637.15 \pm 0.06$
$\mu_2 = -6763.30 \pm 907539835.51$
$\sigma_1 = -24.42 \pm 0.05$
$\sigma_2 = -289097.60 \pm 41751769508.43$
$a = 2201.22 \pm 65542.17$ counts
$b = -2.38 \pm 0.02$ counts/channel
$\chi^2 = 4814.95$
$N = 317$ (dof)
$\chi^2/N = 15.19$
Fit
Data in fit
Counts
Channel

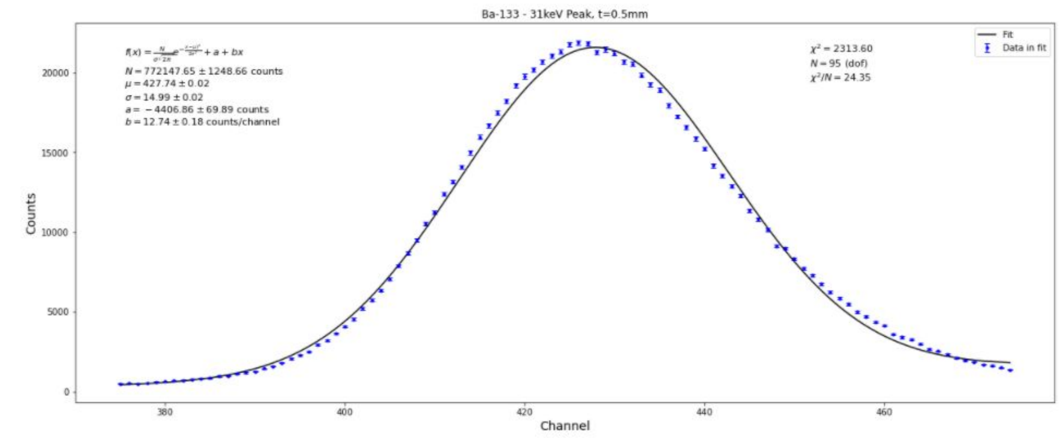
Ba-133 - 31keV Peak, t=0.5mm
$N = 772147.65 \pm 1248.66$ counts
$\mu = 427.74 \pm 0.02$
$\sigma = 14.99 \pm 0.02$
$a = -4406.86 \pm 69.89$ counts
$b = 12.74 \pm 0.18$ counts/channel
$\chi^2 = 2313.60$
$N = 95$ (dof)
$\chi^2/N = 24.35$
Fit
Data in fit
Counts
Channel

x=0mm:

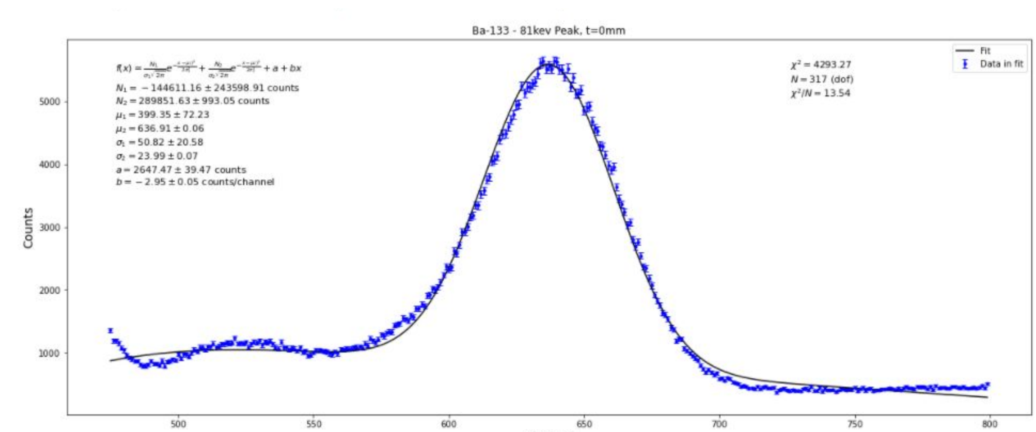
Ba-133 - 81kev Peak, t=0mm
$N_1 = -144611.16 \pm 243598.91$ counts
$N_2 = 289851.63 \pm 993.05$ counts
$\mu_1 = 399.35 \pm 72.23$
$\mu_2 = 636.91 \pm 0.06$
$\sigma_1 = 50.82 \pm 20.58$
$\sigma_2 = 23.99 \pm 0.07$
$a = 2647.47 \pm 39.47$ counts
$b = -2.95 \pm 0.05$ counts/channel
$\chi^2 = 4293.27$
$N = 317$ (dof)
$\chi^2/N = 13.54$
Fit
Data in fit
Counts
Channel

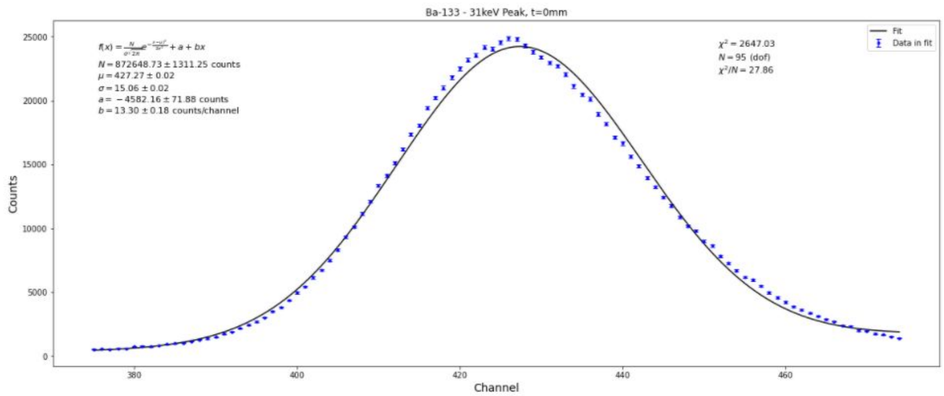

As can be seen, the Gaussians are less of a good fit for these very low thicknesses. From the 81keV plots, we can see that there is a smaller ‘peak’ at around channel 525, which wasn’t nearly as apparent in the plots for the larger thicknesses. This Compton shelf certainly complicated the fit and made an accurate one more difficult. The fact that the peak sizes were so much larger for the thinner absorbers than for the thicker absorbers also increased the uncertainty of each reading, since uncertainty was given by the square root of the count number. Having made plots of each peak for all eight thicknesses, it became easier to see the relationships for each peak as thickness changed.

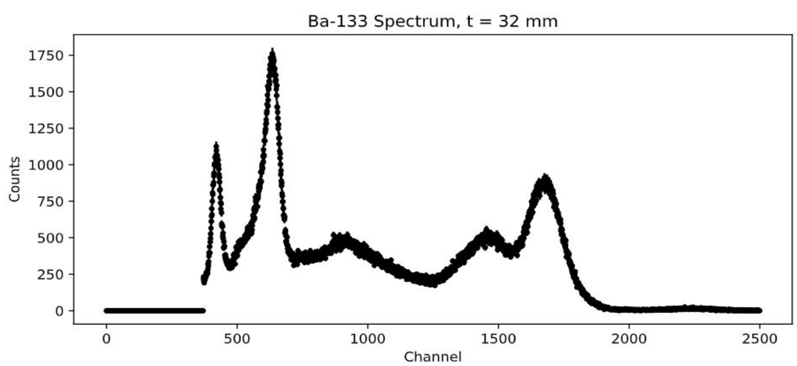

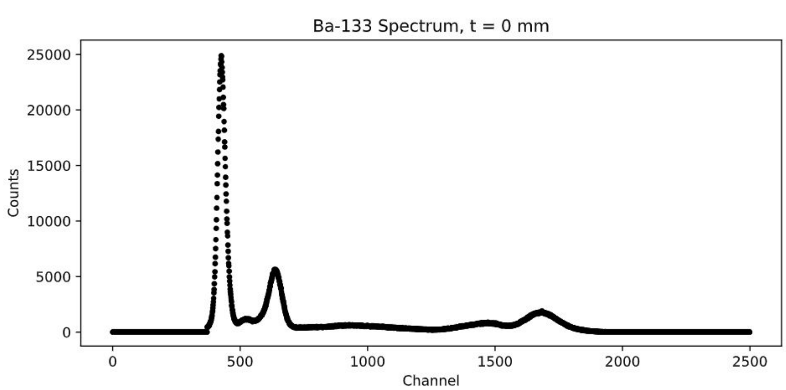

We also had an idea of the relationships between thicknesses for each peak's count rate from the preliminary plots of the raw data from the MCA (above), which show how the first peak increases drastically as the absorber's thickness increased, and how the second peak also increases, but much less significantly. To obtain the true relationships for each peak's count rate to thickness of absorber, we plotted the values of thickness in mm against the count rate (gross counts divided by the livetime of 600 seconds). Using python's fit function, this resulted in the exponential decay curves presented below:

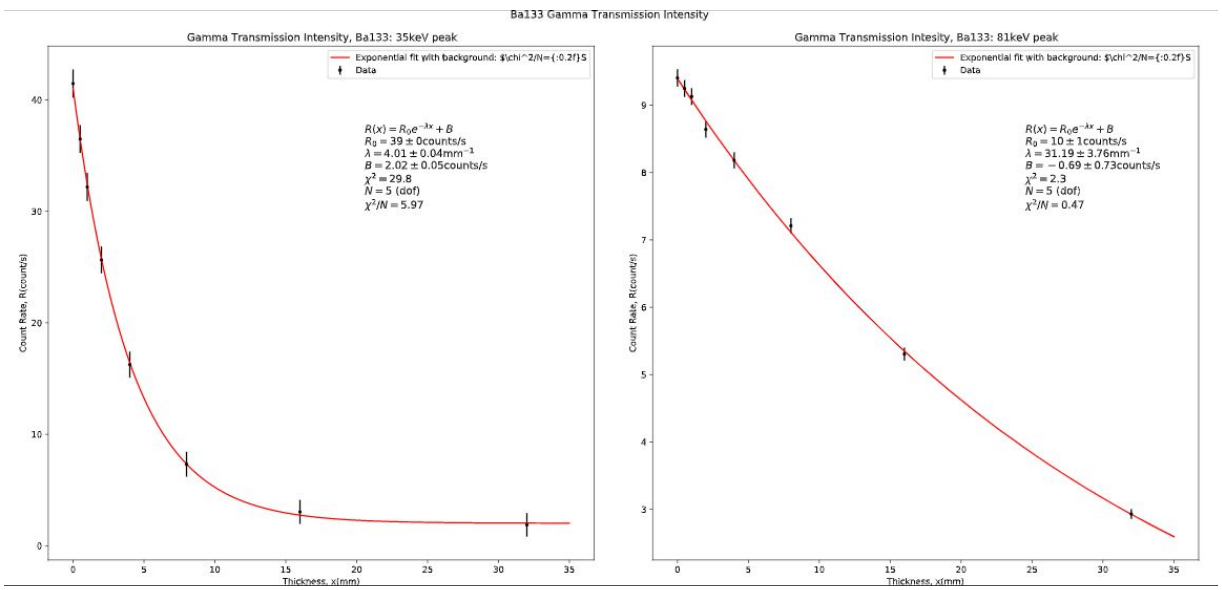

From these graphs, we can see that the 35keV peak had a much more rapidly decaying count rate as thickness increased, but then flattened out. On the other hand, the 81keV peak's count rate decayed much more smoothly. The final values obtained for the linear attenuation coefficient were:

$\mu_l(35keV) = 4.01 \pm 0.04gmm^{-1}$ and

$\mu_l(81keV) = 31.19 \pm 3.76gmm^{-1}$.

Multiplying these values by the atomic number density value for aluminium ($\rho_A =$ $2.70\, gcm^{-3}$ or $2.71 \times 10^3 gmm^{-3}$), we obtain the following best estimate cross-section values:

$\sigma_T(35keV) = (1.09 \pm 0.01) \times 10^4\ mm^2$ and

$\sigma_T(81keV) = (8.45 \pm 1.02) \times 10^4 mm^2$.

Conclusion

It would be best to compare the obtained values to a physics literary source but, although we arrived at the determination of the two desired cross-section values, it is difficult to find a literature source for the cross-sections at the same energies as were investigated. In order to improve the accuracy of the measured values, we could have taken longer to collect data for each thickness of absorber. The uncertainty in the cross-section value would still be the same, however, since it comes from our determination of the mass attenuation coefficient and is dependent on the count rate. The precision of the final value may be increased by increasing the number of bins (channels) that the multichannel analyser could discriminate the inputs into, but this may not be possible as it is a limitation of the equipment used in the experiment. Of course increasing the number of different absorbers for which we take data would improve the accuracy of determination of the mass attenuation coefficients, and thus of the final cross-sections. There was, however, a limit on both the time for which we could take data on each absorber, and on the number of absorbers available for use through the Red Pitaya.